



Title	Development of achromatic full-field hard X-ray microscopy and its application to X-ray absorption near edge structure spectromicroscopy
Author(s)	Matsuyama, S.; Emi, Y.; Kino, H. et al.
Citation	Proceedings of SPIE – The International Society for Optical Engineering. 2014, 9207, p. 92070Q
Version Type	VoR
URL	https://hdl.handle.net/11094/86943
rights	Copyright 2014 SPIE. One print or electronic copy may be made for personal use only. Systematic reproduction and distribution, duplication of any material in this publication for a fee or for commercial purposes, or modification of the contents of the publication are prohibited.
Note	

The University of Osaka Institutional Knowledge Archive : OUKA

<https://ir.library.osaka-u.ac.jp/>

The University of Osaka

Development of achromatic full-field hard X-ray microscopy and its application to X-ray absorption near edge structure spectromicroscopy

S. Matsuyama^{*a}, Y. Emi^a, H. Kino^a, Y. Kohmura^b, M. Yabashi^b, T. Ishikawa^b, K. Yamauchi^{a,c}

^a Department of Precision Science and Technology, Graduate School of Engineering,
Osaka University, 2-1 Yamada-oka, Suita, Osaka 565-0871, Japan

^b RIKEN/SPring-8, 1-1-1 Kouto, Sayo-cho, Sayo-gun, Hyogo 679-5148, Japan

^c Research Center for Ultra-Precision Science and Technology, Graduate School of Engineering,
Osaka University, 2-1 Yamada-oka, Suita, Osaka 565-0871, Japan

ABSTRACT

An achromatic and high-resolution hard X-ray microscope was developed, in which advanced Kirkpatrick-Baez mirror optics with four total-reflection mirrors was employed as an objective. A fine test pattern with a 100 nm feature size could successfully be resolved. Full-field imaging, in combination with X-ray absorption near edge structure (XANES) spectroscopy, was used to characterize tungsten particles. XANES spectra were obtained over the entire observation area, showing good agreement with the XANES spectrum of pure tungsten.

Keywords: advanced Kirkpatrick-Baez optics, Wolter mirror, full-field X-ray microscopy, X-ray mirror, XANES

1. INTRODUCTION

X-rays have the potential for use in non-destructive elemental and structural analysis. Because of the high penetration depth of hard X-rays, they are also used to analyze the interior of objects and samples in aqueous and/or gaseous environments. Additionally, given their short wavelength, X-ray microscopy can overcome the resolution limit of conventional visible light microscopy. Thus, analytical hard X-ray microscopes that can analyze objects, especially thick objects, at high resolution are useful and can become complementary tools to visible light or electron microscopes, amongst others. From an analytical point of view, a microscope exhibiting achromatism is desirable. However, there are few reports on such achromatic and high-resolution microscopes.

We aim at the realization of an achromatic and high-resolution full-field hard X-ray microscope based on four total reflection mirrors. This design employs advanced Kirkpatrick-Baez (KB) mirror optics¹ and comprises two pairs of elliptical mirrors and hyperbolic mirrors. The optical imaging system is advantageous because the mirror fabrication is possible with a figure error better than 2 nm and a wide field of view (FOV) can be obtained. In contrast, despite enabling a wide FOV, a Wolter mirror^{2,3} is extremely difficult to fabricate. Furthermore, a KB mirror^{4,5}, the fabrication difficulty of which is comparable to that of an advanced KB mirror, does not allow for a wide FOV.

Our approach towards such a microscope is described by the following steps: (I) development of a precise simulator of the imaging system to investigate influences of figure errors and mirror misalignments⁶, (II) mirror fabrication with highest possible accuracy^{7,8}, (III) development of a mirror manipulator to precisely align the mirrors⁸, and (IV) development of a microscope system that includes a condenser and positioner for samples^{9,10}. Currently, these steps have already been completed. In 2013, we started the performance tests of the microscope and observations of practical samples. The details of the performance tests are described elsewhere¹¹. In this study, we observe micron-size particles while characterizing their chemical state by X-ray absorption near edge structure (XANES) spectroscopy^{12,13}.

*matsuyama@prec.eng.osaka-u.ac.jp; phone/fax +81-6-6879-7286; <http://www.dma.jim.osaka-u.ac.jp/view?l=en&u=4001>

2. X-RAY MICROSCOPE

Table 1 lists parameters and specifications of the developed advanced KB mirror optics. A magnification of 658×214 ($V \times H$) is obtained in the BL29XUL¹⁴ of SPring-8 owing to the long distance between the first and third experimental hutches. The achievable minimum spatial resolution, defined as the smallest half-period that can be resolved with a contrast of 26.5% (the Rayleigh criterion¹⁵ for a circular aperture), is found to be 49 nm and 40 nm for partial coherence factors¹⁵ ($\sigma = \text{NA}_{\text{condenser}}/\text{NA}_{\text{objective}}$) of 0 and 1, respectively, by considering only the NA of the objective and σ .

Table 1. Parameters and specifications of the developed advanced KB mirror optics

	M1	M2	M3	M4
	Vertical imaging		Horizontal imaging	
Shape	Hyperbola	Ellipse	Hyperbola	Ellipse
Coating material	Pt	Pt	Pt	Pt
a^* (m)	20.51×10^{-3}	22.57	68.57×10^{-3}	22.66
b^* (m)	0.3111×10^{-3}	13.34×10^{-3}	1.044×10^{-3}	23.60×10^{-3}
Average incident glancing angle (mrad)	5.0	5.5	5.1	5.5
Distance from object (mm)**	50	90	161	268
Mirror length (mm)	30	38	92	111
Magnification factor	658		214	
Numerical aperture	1.51×10^{-3}		1.46×10^{-3}	
Field of view*** (μm)	12		24	
Depth of focus*** (μm)			50	
Working distance (mm)			35	

* Ellipse $x^2/a^2 + y^2/b^2 = 1$ or hyperbola $x^2/a^2 - y^2/b^2 = 1$.

** At the center of the mirror.

*** The values required to obtain 50 nm resolution

A schematic representation of the whole system is shown in Fig. 1. A diffuser consisting of a fine sand paper and a motorized rotational stage is placed most upstream of the microscope system to reduce coherence of incident X-rays and speckle noises. Two plane mirrors in KB configuration are used to adjust the X-ray trajectory, using a grazing-incidence angle of ~ 3 mrad. This is done to assure that the beam direction reflected on the objective mirrors is parallel to the beamline, in order to successfully deliver the X-rays to the image plane, which is placed deep within a long (~ 40 m) and narrow (~ 40 mm as minimum diameter) vacuum duct. Two elliptical mirrors in KB configuration are used to collect X-rays on a sample. The NAs are 2.1×10^{-3} and 1.5×10^{-3} in the vertical and horizontal direction, respectively. The visible light microscope placed just upstream of the sample holder is used to position a sample inside the area of illumination and within the FOV of the objective. This microscope contains a tilted mirror with a hole (diameter of 2 mm) to observe samples without blocking X-rays. The sample holder can hold 6 samples with dimensions (length \times width \times thickness) of $10 \times 10 \times 0.5$ mm³. A fine test pattern (XRESO-100, NTT Advanced Technology Corporation), a cross gold wire with a diameter of 200 μm , a scintillator (YAG:Ce ceramic), as well as samples for XANES spectroscopy were used to adjust the condenser and the objective. To complete the four-mirror alignment, two pairs of laser displacement meters and autocollimators were installed. The adjustment, whose detailed procedure is described in elsewhere⁸, was done with an accuracy of 1 μm and 10 μrad just before beam time. The used X-ray camera system (AA20MOD, Hamamatsu Photonics) consists of a thin scintillator (P43 with a thickness of 10 μm), a relay lens ($\times 2$), and a CCD (ORCA-R2, Hamamatsu Photonics). The CCD has 1344×1024 pixels, each with a size of 6.45 μm . The actual resolution of the camera system is limited to ~ 10 μm due to blurring effects occurring at the scintillator.

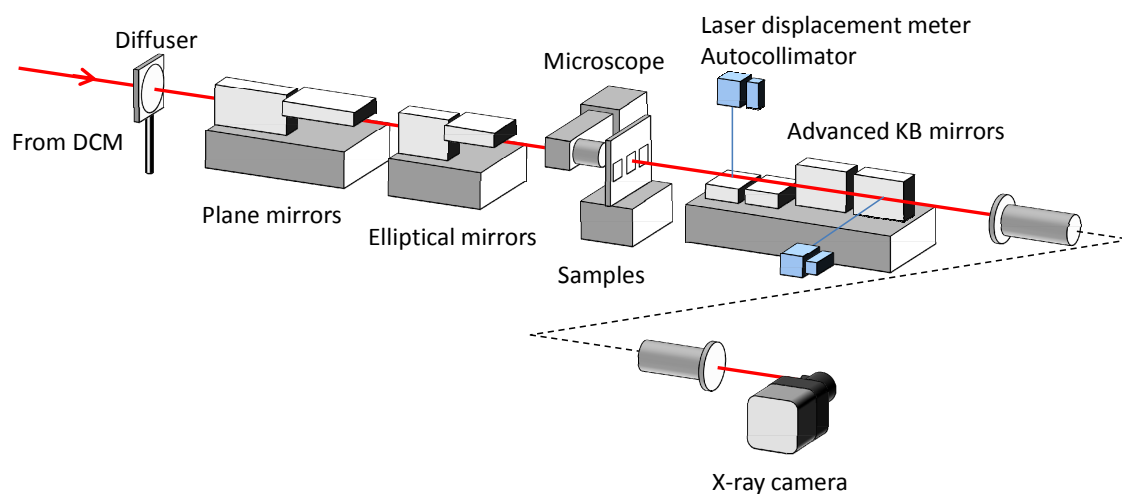


Figure 1. Schematic representation of the X-ray microscope system.

3. EXPERIMENTS AND RESULTS

Before starting the observation and spectroscopic measurements of tungsten particles, the condenser and the objective were carefully adjusted. To facilitate adjustments related to sample positioning and the determination of the FOV center, the condenser was used in a defocused state. The obtained illumination area was approximately $30 \times 160 \mu\text{m}^2$ ($V \times H$). The focus and FOV center were adjusted observing the test pattern. Fig. 2 shows a bright-field image of this test pattern, which is made of tantalum, and has its finest 100 nm feature at its innermost side, where the thickness is $1 \mu\text{m}$. The used energy is 9.881 keV, which corresponds to an energy just above the absorption edge of tantalum. The data analysis includes a flat field correction, in which the obtained image data are normalized by image data taken in the absence of a sample, and a magnification correction, in which an image distorted by mismatched magnifications is corrected in order to have a real aspect ratio. As can be seen in Fig. 2, 100 nm features can be resolved.

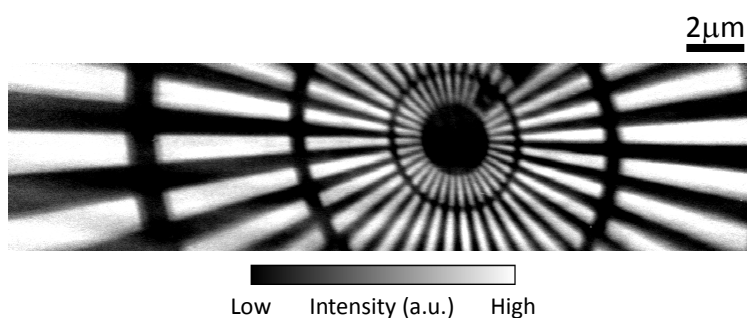


Figure 2. Bright-field image of the test pattern. The innermost side has a 100 nm line width. The used energy is 9.881 keV and the exposure time is 30 s.

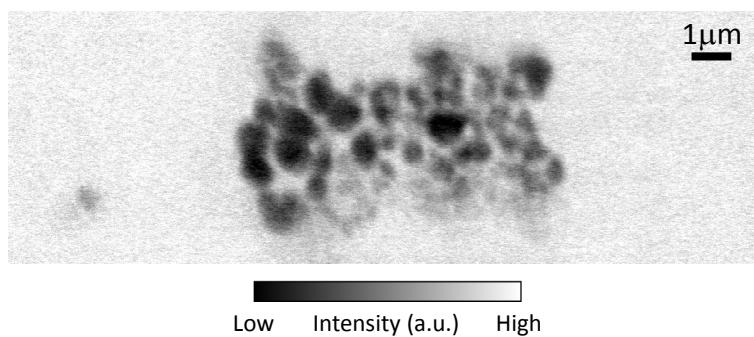


Figure 3. Bright-field image of tungsten particles. The used energy is 10.204 keV and the exposure time is 30 s.

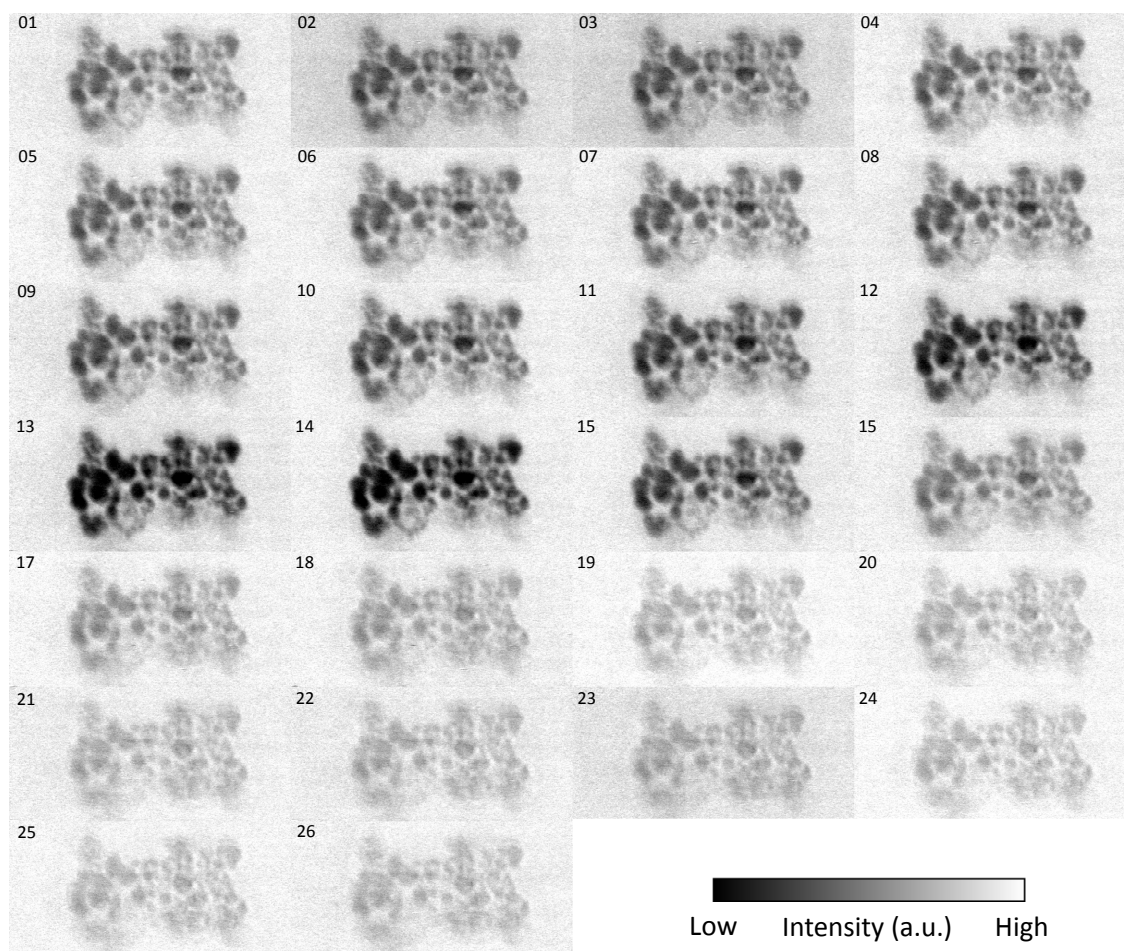


Figure 4. Overview of a series of images used for XANES spectra. The image labeled “01” is the first image taken at an energy of 10230 eV, while the one labeled “26” corresponds to the last image taken at an energy of 10180 eV. The exposure time for every image is 30 s.

As a first test of a practical observation, imaging XANES spectroscopy on fine particles was carried out. The analyzed sample consisted of tungsten particles (W-1K, JAPAN NEW METALS CO., LTD) with diameters of $0.60 - 0.99 \mu\text{m}$ and a purity of $>99.9\%$, which were sprayed on a 270 nm thick SiN membrane (MEM-N020027/10M, NTT Advanced Technology Corporation). Approximately one million XANES spectra were acquired using the following procedure. First, 26 images were taken at different energies ranging from 10230 to 10180 eV . During these measurements, images without samples were taken once every 5 shots for the flat field correction. After all measurements, the data were corrected by the methods discussed above. The flat field correction was done using the reference image data without samples that were captured nearest in time. The obtained X-ray intensity data were converted to an absorption parameter expressed as μt , in which μ is the linear absorption coefficient and t is the thickness of the sample. The XANES spectra of interest were then plotted as a function of the X-ray energy. At this point, the spectra showed much data variation, since the motorized XZ stage supporting the samples, which is used for sample selection and to take images without samples, had a positioning error of $\sim 200 \text{ nm}$ even after removal of the backlash. This positioning error was corrected with the phase correlation method¹⁶, which is a kind of image registration method. Fig. 3 shows the image taken at 10204 eV , which corresponds to an energy just above the absorption edge of tungsten, while Fig. 4 is an overview of all the images after the correction. Fig. 5 shows experimental XANES spectra of certain particles. The spectra were averaged over a $145 \times 145 \text{ nm}^2$ square area. The dashed line represents a reference spectrum of pure tungsten, which was obtained from Fig. 2 of the article *published by Uo et al.*¹⁷. The comparison shows that the experimental spectra are in good agreement with the spectrum of pure tungsten.

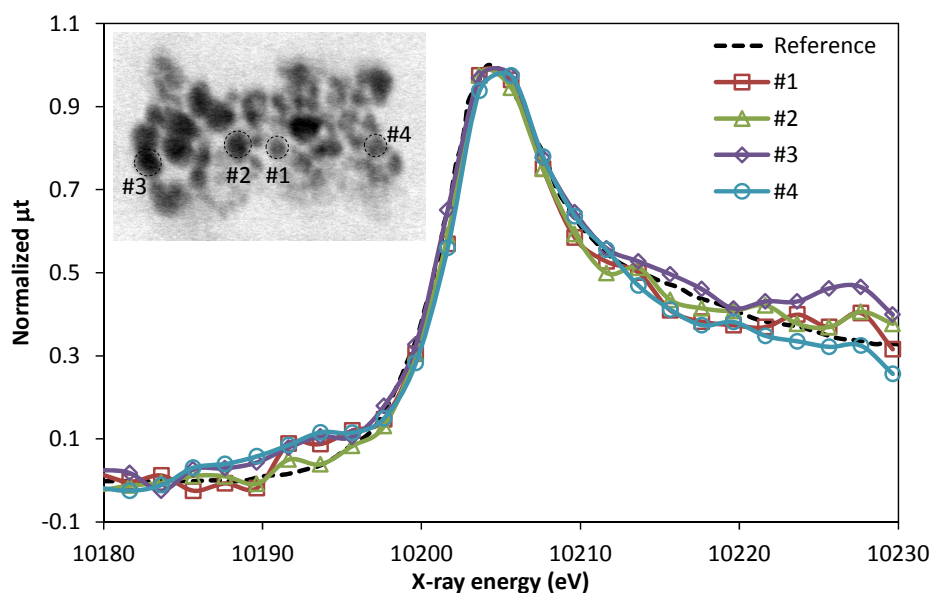


Figure 5. XANES spectra of tungsten particles. The spectra labeled #1 to #4 correspond to spectra taken at the particle centers. The spectra were averaged over a $145 \times 145 \text{ nm}^2$ square area. The spectrum named “Reference” is a reference spectrum of pure tungsten, which was obtained from Fig. 2 of the article *published by Uo et al.*¹⁷.

4. SUMMARY AND OUTLOOK

We developed an achromatic and high-resolution hard X-ray microscope based on total-reflection mirrors. Observation of the test pattern demonstrated that 100 nm features could be visualized. Full-field imaging combined with XANES spectroscopy was used to characterize tungsten particles, showing that approximately one million XANES spectra could successfully be obtained over the entire observation area. Although this first test was successful, some problems remain to be overcome. One of them is related to the stability of both the objective and the condenser consisting of multiple mirrors. In this regard, the relative alignment between the elliptical mirror and the hyperbolic mirror in the objective

suffered gradual changes, resulting in blurred images. Besides, also the intensity distribution of the illumination, which is produced by the condenser, showed gradual changes. Therefore, the stability of the entire optical system should be improved. The other problem relates to the accuracy of the translation stage that supports the samples, which caused data variation in the XANES spectra. To overcome this problem, a closed-loop positioning system based on a linear encoder should be installed on this stage. Next to the full-field XANES spectromicroscope, we have also developed a full-field X-ray fluorescence microscope that can create colorful images of X-rays emitted from an object using a photon-counting area detector. Such a microscope would become a powerful tool for the observation of elemental distributions in samples.

ACKNOWLEDGEMENTS

This research was supported by the SENTAN project of JST. It was partially supported by JSPS KAKENHI (Grant Nos. 26286077, 23226004), the CREST project of JST, and the Global COE program (H08) from MEXT. The use of BL29XUL at SPring-8 was supported by RIKEN. We would like to acknowledge JTEC Corporation for helping with the substrate processing.

REFERENCES

- [1] Kodama, R., Ikeda, N., Kato, Y., Katori, Y., Iwai, T., and Takeshi, K., "Development of an advanced Kirkpatrick-Baez microscope," *Opt. Lett.* 21(17), 1321–1323 (1996).
- [2] Wolter, H., "Glancing incidence mirror systems as imaging optics for X-rays," *Ann. Phys.* 10, 94–114 (1952).
- [3] Hasegawa, M., Taira, H., Harada, T., Aoki, S., and Ninomiya, K., "Fabrication of Wolter-type x-ray focusing mirror using epoxy resin," *Rev. Sci. Instr.* 65(8), 2568 (1994).
- [4] Kirkpatrick, P., and Baez, A. V., "Formation of optical images by X-Rays," *J. Opt. Soc. Am.* 6(1895), 766–774 (1946).
- [5] Mimura, H., Matsuyama, S., Yumoto, H., Hara, H., Yamamura, K., Sano, Y., Shibahara, M., Endo, K., Mori, Y., Nishino, Y., Tamasaku, K., Yabashi, M., Ishikawa, T., and Yamauchi, K., "Hard X-ray diffraction-limited nanofocusing with Kirkpatrick-Baez mirrors," *Jpn. J. Apply. Phys.* 44(18), L539–L542 (2005).
- [6] Matsuyama, S., Fujii, M., and Yamauchi, K., "Simulation study of four-mirror alignment of advanced Kirkpatrick–Baez optics," *Nucl. Instrum. Methods Phys. Res., Sect. A* 616(2-3), 241–245 (2010).
- [7] Matsuyama, S., Wakioka, T., Kidani, N., Kimura, T., Mimura, H., Sano, Y., Nishino, Y., Yabashi, M., Tamasaku, K., Ishikawa, T., and Yamauchi, K., "One-dimensional Wolter optics with a sub-50 nm spatial resolution," *Opt. Lett.* 35(21), 3583–3585 (2010).
- [8] Matsuyama, S., Kidani, N., Mimura, H., Sano, Y., Kohmura, Y., Tamasaku, K., Yabashi, M., Ishikawa, T., and Yamauchi, K., "Hard-X-ray imaging optics based on four aspherical mirrors with 50 nm resolution," *Opt. Express* 20(9), 10310–10319 (2012).
- [9] Matsuyama, S., Emi, Y., Kino, H., Sano, Y., Kohmura, Y., Tamasaku, K., Yabashi, M., Ishikawa, T., and Yamauchi, K., "Development of achromatic full-field x-ray microscopy with compact imaging mirror system," *Proc. SPIE* 8851, 885107–885108 (2013).
- [10] Matsuyama, S., Emi, Y., Kohmura, Y., Tamasaku, K., Yabashi, M., Ishikawa, T., and Yamauchi, K., "Development of achromatic full-field hard X-ray microscopy using four total-reflection mirrors," *J. Phys.: Conf. Ser.* 463, 012017 (2013).
- [11] Matsuyama, S., Emi, Y., Kino, H., Kohmura, Y., Yabashi, M., Ishikawa, T., and Yamauchi, K., "Achromatic and high-resolution full-field X-ray microscopy based on total-reflection mirrors," manuscript in preparation.
- [12] Meirer, F., Cabana, J., Liu, Y., Mehta, A., Andrews, J.C., and Pianetta, P., "Three-dimensional imaging of chemical phase transformations at the nanoscale with full-field transmission X-ray microscopy," *J. Synchrotron Radiat.* 18, 773–781 (2011).
- [13] Fayard, B., Pouyet, E., Berruyer, G., Bugnazet, D., Cornu, C., Cotte, M., Andrade, V. De, Chiaro, F. Di, Hignette, O., Kieffer, J., Martin, T., Papillon, E., Salomé, M., and Sole, V. A., "The new ID21 XANES full-field end-station at ESRF," *J. Phys.: Conf. Ser.* 425(19), 192001 (2013).

- [14] Tamasaku, K., Tanaka, Y., Yabashi, M., Yamazaki, H., Kawamura, N., Suzuki, M., and Ishikawa, T., “SPring-8 RIKEN beamline III for coherent X-ray optics,” Nucl. Instrum. Methods Phys. Res., Sect. A 467-468, 686–689 (2001).
- [15] Born, M. and Wolf, E., [Principles of Optics 7th ed.], Cambridge University Press (1999).
- [16] Stone, H.S., Orchard, M.T., and Martucci, S.A., “A fast direct Fourier-based algorithm for subpixel registration of images,” IEEE Trans. Geosci. Remote Sens. 39(10), 2235–2243 (2001).
- [17] Uo, M., Asakura, K., Watanabe, K., and Watari, F., “XAFS analysis of the bronchoalveolar lavage fluid of a tungsten carbide pneumoconiosis patient,” Chem. Lett. 39(8), 852–853 (2010).